ACS Biomaterials SCIENCE & ENGINEERING
Cite This: ACS Biomater. Sci. Eng. XXXX, XXX, XXX−XXX
Article
pubs.acs.org/journal/abseba

Chiral Recognition of Lipid Bilayer Membranes by Supramolecular Assemblies of Peptide Amphiphiles

Kohei Sato,[†,‡,△] Wei Ji,[‡,§,∥] Zaida Álvarez,[‡] Liam C. Palmer,[†,‡] and Samuel I. Stupp*[,†,‡,⊥,#,¶]

[†]Department of Chemistry, [⊥]Department of Materials Science and Engineering, and [¶]Department of Biomedical Engineering, Northwestern University, Evanston, Illinois 60208, United States

[‡]Simpson Querrey Institute and [#]Department of Medicine, Northwestern University, Chicago, Illinois 60611, United States

[§]Prometheus, Division of Skeletal Tissue Engineering and [∥]Skeletal Biology and Engineering Research Center, Department of Development and Regeneration, Katholieke Universiteit Leuven, Leuven 3000, Belgium

Supporting Information

ABSTRACT: On the basis of the exclusive existence of homochirality in biomolecules and the well-known phenomenon of chiral recognition, it is obvious that chirality is a crucial factor in biological events. We report here that supramolecular assemblies of peptide amphiphiles interact with lipid bilayer membranes in a stereospecific manner. When negatively charged chiral phospholipid bilayer vesicles were subjected to the assemblies, we found that peptide amphiphiles with L-amino acids show stronger affinity for the liposomes compared to the ones with D-amino acids. To examine their biological functions, we tested the cytotoxicity of nanofibers against mammalian primary cells using human bone marrow mesenchymal stem cells and murine astroglial cells. We demonstrated that cell viability increased when D-amino acids were incorporated in the structure of peptide amphiphiles, which is consistent with our finding of their weaker interactions with lipid bilayer membranes.

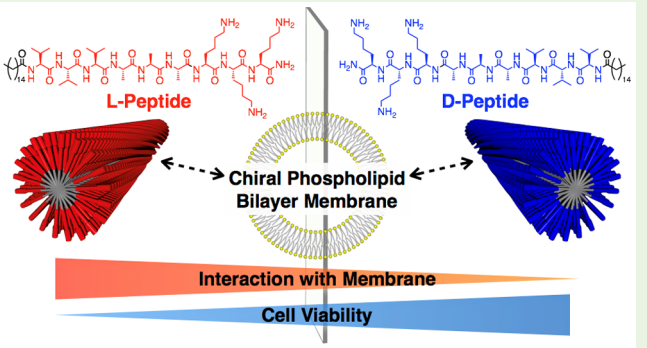

KEYWORDS: *supramolecular assembly, peptide amphiphile, lipid bilayer membrane, chiral recognition, mammalian primary cells*

INTRODUCTION

Since the discovery of optical resolution of sodium ammonium tartrate by Pasteur,[1] chirality has been one of the most intriguing topics in science.[2] Chirality is a crucial factor in all fundamental biological events because essential biomolecules such as proteins, lipids, nucleic acids, and saccharides are all strongly biased to a single chirality.[3] In fact, it has been reported that cells show different biological response depending on the chirality of matrices in which they are cultured.[4−15] L- and D-amino acid-functionalized surfaces and peptide-based materials are often used in these studies, because of their availability and well-established synthetic strategies. Some studies have demonstrated a preference for proteins to adhere to surfaces formed by a single enantiomer of chiral self-assembling monolayers and nanofibers.[9,16−18] This then led to a difference in cell adhesion and differentiation, but we still lack a full chemical understanding of how chirality affects biological events.

Supramolecular polymers are particularly useful materials to study chiral recognition, since the chirality of their constituent monomers can be amplified over larger length scales, for example, in the twisted morphologies of supramolecular assemblies.[2f,g] Moreover, supramolecular interactions are an integral part of many biological events. In this regard, the lipid bilayer membranes of cells are formed by supramolecular self-assembly of chiral lipid molecules.[3c] In fact, some low molecular-weight chiral compounds, such as amino acids and dipeptides, were reported to interact with chiral lipid bilayer membranes in a stereospecific manner.[19] The goal of this work has been to explore the interactions between chiral supramolecular polymers and chiral supramolecular assemblies in biological systems. We were not able to find any detailed studies on such interactions, and thus proceeded to study them using the well-known supramolecular assemblies formed by chiral peptide amphiphiles (PA). Our laboratory has extensively studied the supramolecular self-assembly of PAs and more recently their molecular dynamics.[20,21] The PAs developed by our laboratory are molecules in which a hydrophobic alkyl tail is covalently linked to an amino acid sequence that promotes the formation of supramolecular nanofibers.[20b] These assemblies have been of great interest for their potent ability to signal cells and create artificial extracellular matrices suitable for regenerative medicine.[22−26] In this work, we designed and synthesized PAs with variable

Received: April 19, 2019
Accepted: May 16, 2019

DOI: 10.1021/acsbiomaterials.9b00553
ACS Biomater. Sci. Eng. XXXX, XXX, XXX−XXX

amino acid stereochemistry, and investigated their potential for chiral recognition in biology, particularly their interaction with lipid bilayer membranes and cells.

RESULTS AND DISCUSSION

Figure 1a shows the molecular structures of four PAs with variations in amino acid chirality in their charged terminus

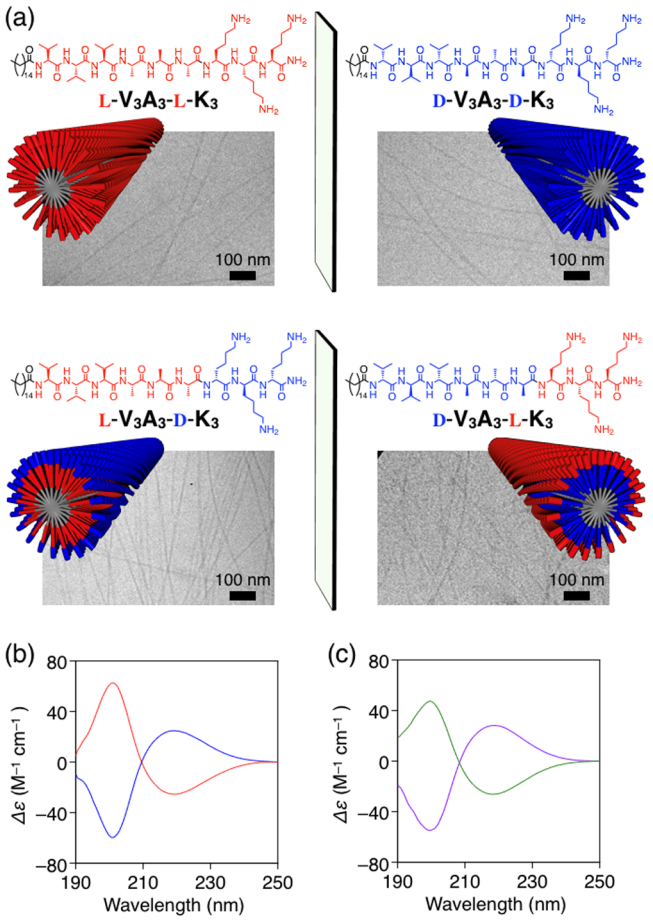

Figure 1. (a) Schematic molecular structures, cryogenic TEM micrographs in H_2O ([PA] = 440 μM), and illustrations of supramolecular assemblies of **L-V_3A_3-L-K_3**, **D-V_3A_3-D-K_3**, **L-V_3A_3-D-K_3**, and **D-V_3A_3-L-K_3** forming cylindrical nanofibers. L- and D-amino acids are colored in red and blue, respectively. Supramolecular chirality is determined by β-sheet forming domains (V_3A_3: valine-valine-valine-alanine-alanine-alanine). (b, c) Circular dichroism (CD) spectra of (b) **L-V_3A_3-L-K_3** (red curve) and **D-V_3A_3-D-K_3** (blue curve), and (c) **L-V_3A_3-D-K_3** (green curve) and **D-V_3A_3-L-K_3** (purple curve) at 25 °C in aqueous NaCl ([NaCl] = 10 mM) ([PA] = 220 μM.

(K_3) and β-sheet-forming domain (V_3A_3). **L-V_3A_3-L-K_3** is exclusively composed of natural L-amino acids and has been extensively studied by our group.[21b,27] **D-V_3A_3-D-K_3** is an enantiomer of **L-V_3A_3-L-K_3** and should therefore have very similar physical properties to **L-V_3A_3-L-K_3**. **L-V_3A_3-D-K_3** is a diastereomer of **L-V_3A_3-L-K_3** and **D-V_3A_3-D-K_3** in which the charged terminus (K_3) is composed of D-amino acids but its β-sheet-forming domain (V_3A_3) consists of natural L-amino acids. **D-V_3A_3-L-K_3** is an enantiomer of **L-V_3A_3-D-K_3**, where its K_3 sequence is composed of L-amino acids, whereas the V_3A_3 domain consists of D-amino acids. Because the V_3A_3 domain has previously been shown to be responsible for the formation of intermolecular hydrogen bonds,[21b,27] we hypothesized that the molecular chirality of the V_3A_3 domain would dictate the supramolecular chirality of the assemblies formed in aqueous media.

PAs **L-V_3A_3-L-K_3**, **L-V_3A_3-D-K_3**, **D-V_3A_3-L-K_3**, and **D-V_3A_3-D-K_3** were synthesized through solid-phase peptide synthesis, and their purity was confirmed by analytical HPLC and ESI mass spectrometry (Figures S1−S8). Cryogenic transmission electron microscopy (cryo-TEM) revealed the formation of high-aspect-ratio nanofibers for all PAs with lengths of up to several micrometers (Figure 1a). Solution-phase small-angle X-ray scattering (SAXS) showed scattering curves with a slope of −1 in the low-q region for all PAs, which are typical of nanofibers (Figure S9). Fourier-transform infrared spectroscopy (FT-IR) of film samples showed stretching vibrations due to amide I at 1628 cm^{-1}, which are typical of peptides with β-sheet secondary structures (Figure S10).[28] To assess the chirality of the assemblies, we carried out circular dichroism (CD) spectroscopy measurements of PA solutions in aqueous NaCl ([NaCl] = 10 mM) (Figure 1b, c). Consistent with our previous reports,[21b] **L-V_3A_3-L-K_3** revealed a negative Cotton peak at 220 nm and a positive Cotton peak at 200 nm, indicating that the assembly in solution is rich in β-sheet peptide configurations (Figure 1b, red curve). As expected, **D-V_3A_3-D-K_3** showed a mirror image signal of **L-V_3A_3-L-K_3** (Figure 1b, blue curve). Meanwhile, **L-V_3A_3-D-K_3**, whose headgroup is composed of D-amino acids whereas its β-sheet-forming domain consists of L-amino acids, effectively showed the same CD signal as **L-V_3A_3-L-K_3** (Figure 1c, green curve). Likewise, **D-V_3A_3-L-K_3** showed a CD signal similar to that of **D-V_3A_3-D-K_3** (Figure 1c, purple curve). These results indicate that the chiral secondary structure of PA assemblies is determined by the molecular chirality of amino acids within the β-sheet forming domain. We propose that the PA molecules adopt a slightly twisted arrangement within cylindrical nanofibers, which is consistent with the β-sheet twisting observed in proteins in nature (Figure 1a).[29]

Under aqueous conditions, amine groups are known to interact with negatively charged groups such as carboxylic acids and phosphates through the formation of salt-bridges.[30] Because mammalian cell membranes are slightly negatively charged and their constituent phospholipids have exclusively R configuration,[3c] we anticipated that PA fibers potentially interact with lipid bilayer membranes in a stereospecific manner. We reported previously that PA fibers with a length of a few hundred nanometers seemed to damage lipid bilayer membranes through interactions with their fiber termini, whereas those with the length up to micrometers did not.[21b,31] Therefore, in this work, we used micrometer-long PA fibers to investigate the interaction between PA fibers of controlled chirality with membranes. As a simplified model of mammalian cell membranes, we selected the coassembled lipid bilayer liposomes of 1-palmitoyl-2-oleoyl-*sn*-glycero-3-phosphocholine (POPC) and 1-palmitoyl-2-oleoyl-*sn*-glycero-3-phospho-L-serine (POPS) (POPC/POPS = 80/20) (Figure 2a).[32,33] Using cryo-TEM and dynamic light scattering, the POPC/POPS liposomes were characterized as mostly unilamellar with an average diameter of 100 nm (Figures S11 and S12). As soon as we mixed the PA fibers with the POPC/POPS liposomes, precipitation was observed. On the other hand, mixtures of PA fibers with neutral POPC liposomes did not form any precipitates. These results indicate that PA fibers are interacting with lipid membranes through electrostatic forces

DOI: 10.1021/acsbiomaterials.9b00553
ACS Biomater. Sci. Eng. XXXX, XXX, XXX−XXX

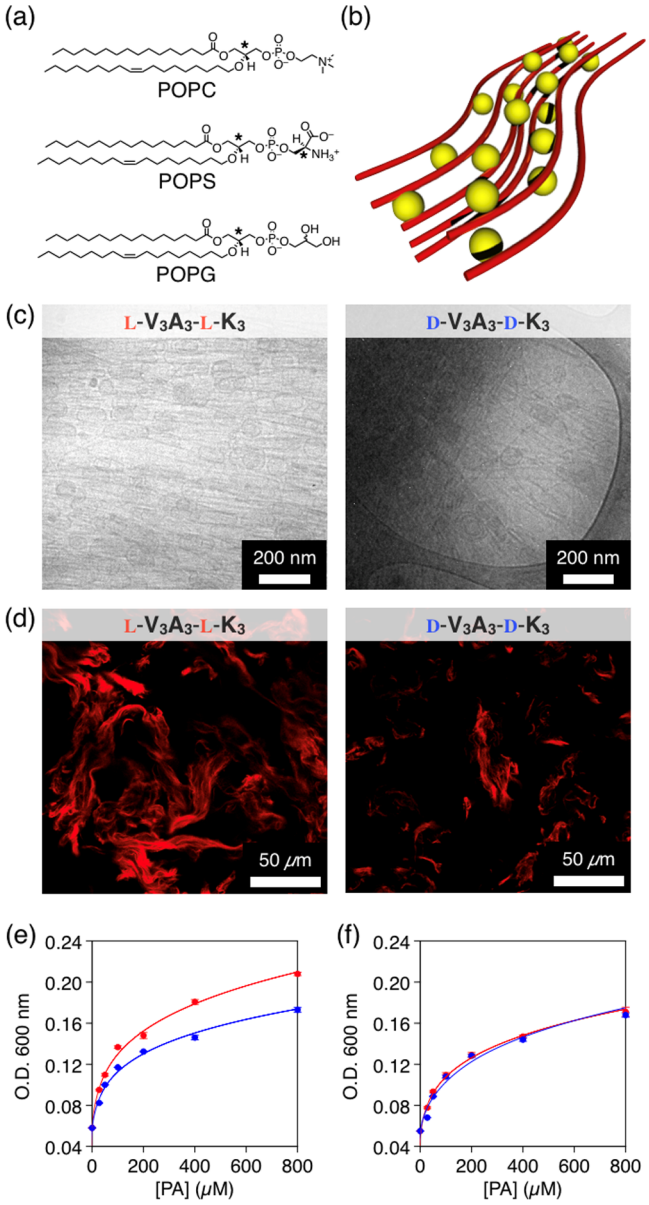

Figure 2. (a) Chemical structures of phospholipids POPC, POPS, and POPG. (b) Schematic illustration of a mixture of positively charged PA fibers (red) and negatively charged liposomes (yellow) to form bundled structures. (c) Cryogenic TEM micrographs of **L-V_3A_3-L-K_3** and **D-V_3A_3-D-K_3** fibers ([PA] = 610 μM) treated with POPC/POPS (80/20) liposomes ([POPC] + [POPS] = 910 μM) in HEPES buffer ([HEPES] = 10 mM, [NaCl] = 100 mM, pH 7). (d) Confocal laser scanning micrographs of **L-V_3A_3-L-K_3** and **D-V_3A_3-D-K_3** fibers ([PA] = 2.3 mM) treated with $DiIC_{18}$(3)-DS-embedded POPC/POPS (80/20) liposomes ([$DiIC_{18}$(3)-DS] = 67 μM, [POPC] + [POPG] = 6.7 mM) in HEPES buffer ([HEPES] = 10 mM, [NaCl] = 100 mM, pH 7) at 25 °C. (e) and (f) Optical densities (O.D.) at 600 nm of suspensions containing PAs (**L-V_3A_3-L-K_3**: red curve; **D-V_3A_3-D-K_3**: blue curve) treated with POPC/POPS (80/20) liposomes ([POPC] + [POPS] = 910 μM) (e), POPC/POPG (80/20) liposomes ([POPC] + [POPG] = 910 μM) (f), both in HEPES buffer ([HEPES] = 10 mM, [NaCl] = 100 mM, pH 7) at 25 °C. Bars represent the standard deviation of the mean.

between the positively charged PA fibers and the negatively charged POPC/POPS liposomes (Figure 2b). We performed cryo-TEM to visualize the aggregates formed with PA fibers and POPC/POPS liposomes. Regardless of the combination of amino acid chirality within the PA structures, the mixtures showed highly bundled fibers coexisting with spherical liposomes (Figure 2c). Previously, our group investigated the molecular interaction between weakly cohesive **$A_3G_3K_3$** PAs and phospholipids by means of differential scanning calorimetry (DSC).[27] Similar to **$V_3A_3K_3$** PAs, **$A_3G_3K_3$** formed nanofibers in aqueous media but acted as cell-penetrating peptides,[34] thus showing high cytotoxicity. In that system, we observed that the phase transition temperature of dipalmitoylphosphatidylcholine (DPPC) lipid membranes decreases in the presence of membrane-incorporating **$A_3G_3K_3$** PAs (Figure S13). In contrast, we performed DSC measurements of DPPC, and found that none of the stereoisomers of **$V_3A_3K_3$** induced any changes in the phase transition temperature of DPPC (Figure S13),indicating that the PA monomers of **$V_3A_3K_3$** had not been incorporated into the DPPC membrane to any significant extent. Although the integrity of DPPC membranes is different from that of POPC/POPS membranes, the DSC results are consistent with cryo-TEM observations that showed PA molecules do not change the structure and size of POPC/POPS liposomes (Figure 2c). Therefore, we concluded that the interaction between PAs and POPC/POPS lipid membranes seems to occur between the surface of PA nanofibers and POPC/POPS liposomes, rather than molecular interactions between monomeric PAs and phospholipids. Furthermore, we prepared fluorescent dye ($DiIC_{18}$(3)-DS)-embedded POPC/POPS liposomes and treated them with PA fibers to visualize the formation of complexes by confocal laser scanning microscope (Figure 2d).[35] Remarkably, **L-V_3A_3-L-K_3** showed the formation of bundles with a width of tens of micrometers while **D-V_3A_3-D-K_3** showed fewer numbers of bundles with lower fluorescence intensity (Figure 2d). We tried a variety of spectroscopic and thermometric analyses to quantify the interaction between PA fibers and POPC/POPS liposomes, however, the strong tendency to precipitate made the measurements hard to interpret. Instead we quantified the amount of precipitate based on light scattering intensity (optical density) at 600 nm (O.D. 600 nm), which is widely used to quantify bacterial growth in microbiology.[36,37] Quite strikingly, O.D. measurements showed different values depending on the chirality of PAs tested (Figure 2e). Namely, **L-V_3A_3-L-K_3** (Figure 2e, red curve) showed higher O.D. values than **D-V_3A_3-D-K_3** (Figure 2e, blue curve). The 50% effective concentration (EC50) values obtained for **L-V_3A_3-L-K_3** and **D-V_3A_3-D-K_3** were 99.13 μM and 203.61 μM, respectively (see the Supporting Information). These results indicate the possibility of chiral recognition between PA assemblies with L-amino acids, revealing a stronger affinity to (*R*)-phospholipid membranes than PAs with D-amino acids. The tendency observed by O.D. measurements is in a good agreement with the morphological difference observed by confocal laser scanning microscope (Figure 2d) and therefore, we concluded that a strong affinity between (*R*)-phospholipid liposomes and PAs with L-amino acids led to the formation of bundled structures (Figure 2b).

To further investigate the mechanism of the chiral recognition between PA nanofibers and lipid bilayer membranes in detail, we focused on structural details of the phospholipids. POPC is a neutral phospholipid, whereas POPS is a negatively charged one. In terms of their stereochemistry, POPC possesses one chiral center within a glycerol unit, whereas POPS possesses two chiral centers: one chiral center within a glycerol unit and another one within a serine

DOI: 10.1021/acsbiomaterials.9b00553
ACS Biomater. Sci. Eng. XXXX, XXX, XXX−XXX

headgroup (Figure 2a). To identify the chiral center that is crucial for chiral recognition by PA fibers, we tested the coassembled lipid bilayer liposomes of POPC and 1-palmitoyl-2-oleoyl-*sn*-glycero-3-phospho-(1′-*rac*-glycerol) (POPG) (POPC/POPG = 80/20).[33] Similar to POPS, POPG is a negatively charged phospholipid that possesses one chiral center within its headgroup; however, it is a 1:1 mixture of *S* and *R* configurations so we wanted to explore whether it would reduce the chiral effect from the headgroup (Figure 2a). As shown in Figure 2f, O.D. of the mixtures of POPC/POPG liposomes with PAs at 600 nm did not show any significant differences among the chiral PAs tested. These results indicate that the inner glycerol unit does not significantly matter, but the headgroup chirality of POPS lipids is crucial for chiral recognition between PA fibers and POPC/POPS liposomes. Although we still do not completely understand the detailed mechanisms of chiral recognition, we hypothesize that L-serine head groups of POPS lipids might preferentially interact with amine groups of L-lysines on the surface of PA nanofibers.

It is known that phospholipids are one of the most abundant lipids in mammalian cell membranes.[38] Therefore, we further examined the interaction of chiral PA assemblies with primary human bone marrow mesenchymal stem cells (BMSCs) and murine astroglial cells. For that purpose, BMSCs were cultured in the presence of **L-V$_3$A$_3$-L-K$_3$** or **D-V$_3$A$_3$-D-K$_3$** PAs (Figure 3 and Figure S15b). After 72 h, cells cultured with **L-V$_3$A$_3$-L-K$_3$** showed lower viability compared to those in contact with **D-V$_3$A$_3$-D-K$_3$**. The 50% cytotoxicity concentration (CC50) values obtained for **L-V$_3$A$_3$-L-K$_3$** and **D-V$_3$A$_3$-D-K$_3$** were 54.71 and 65.14 μM, respectively (see the Supporting Information). We also cultured murine astroglial cells in the presence of chiral PAs. Although we were not able to determine accurate CC50 values because of gelation in the cell media at PA concentrations higher than 200 μM, we did observe a similar trend in cell viability (Figures S14 and S15a). It is quite intriguing that cell viability decreased as the interaction between PA fibers and lipid bilayer membranes increased. In previous work, preferential adhesion of proteins to self-assembling monolayers or nanofibers formed by L-monomers led to enhanced cell viability.[9,10] Similarly, we demonstrated that PA nanofibers formed by L-amino acids possess stronger affinity for the liposomes compared to those with D-amino acids. However, the observed trends in cell viabilities are different from what has been previously reported. Although the mechanism is not perfectly clear, we confirmed that PA molecules did not change the structure and size of POPC/POPS liposomes (Figure 2c and Figure S13). Similarly, we assume that monomeric PAs were not incorporated into the cell membranes to any significant extent but disrupted the bilayer structure. On the basis of a previously reported mechanism, PA fibers might interact with the surfaces of cell membranes, causing their rupture or loss of integrity and leading to cell death.[39] We therefore hypothesize that cell viability can be affected by contact with PA assemblies with opposite chirality to that in natural lipids. This phenomenon could help us understand how cell membrane integrity at the interface is affected by interactions with heterochiral assemblies.

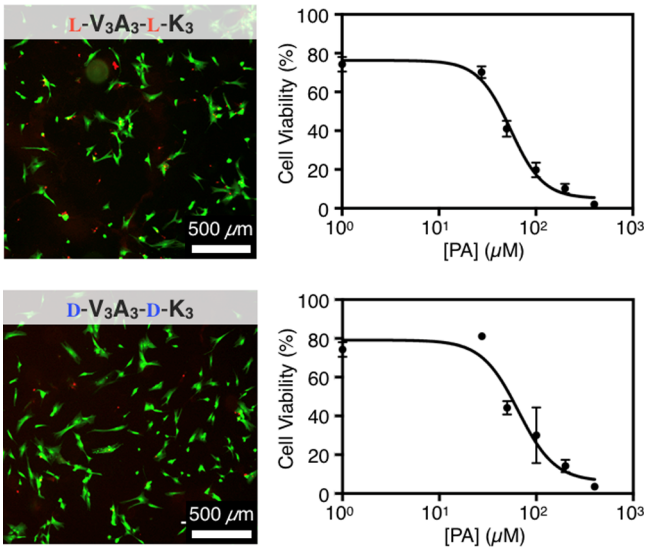

Figure 3. Confocal laser scanning micrographs of human bone marrow mesenchymal stem cells 72 h after treatment with media containing **L-V$_3$A$_3$-L-K$_3$** and **D-V$_3$A$_3$-D-K$_3$** PAs ([PA] = 27.5 μM) using calcein AM (green, live cells) and ethidium-homodimer (red, dead cells) for staining (left), and corresponding quantification of cell viability at different PA concentrations (right). Cell viability was quantified as percentage of live cells (green) in the entire cell population (green + red). Bars represent the standard deviation of the mean.

Finally, we investigated chiral recognition among **L-V$_3$A$_3$-D-K$_3$** and **D-V$_3$A$_3$-L-K$_3$** PA assemblies. Similarly to **L-V$_3$A$_3$-L-K$_3$** and **D-V$_3$A$_3$-D-K$_3$**, **L-V$_3$A$_3$-D-K$_3$** and **D-V$_3$A$_3$-L-K$_3$** formed precipitates when the nanofibers were mixed with POPC/POPS liposomes (Figures S16a and S16b). We measured their O.D. values at 600 nm, and the EC50 values obtained for **L-V$_3$A$_3$-D-K$_3$** and **D-V$_3$A$_3$-L-K$_3$** were 161.02 μM and 182.75 μM, respectively (Figure S16c). Of all the samples, **L-V$_3$A$_3$-L-K$_3$** showed the lowest EC50 value (99.13 μM), whereas **D-V$_3$A$_3$-D-K$_3$** showed the highest EC50 value (203.61 μM). Considering that PA fibers and lipid membranes interact with each other at the interface, the molecular chirality of the K$_3$ terminus is likely to be responsible for chiral recognition. In fact, **L-V$_3$A$_3$-D-K$_3$**, whose K$_3$ charged terminus is composed of D-lysines, showed a weaker affinity for (*R*)-phospholipid membranes relative to **L-V$_3$A$_3$-L-K$_3$**. However, it is interesting that **D-V$_3$A$_3$-L-K$_3$**, whose K$_3$ charged terminus is composed of L-lysines but its inner β-sheet forming domain (V$_3$A$_3$) consists of D-amino acids, showed even weaker affinity to (*R*)-phospholipid membranes relative to **L-V$_3$A$_3$-D-K$_3$**. This observation might imply that the chirality of the β-sheet forming domain plays an important role in chiral recognition among PA fibers and lipid membranes. As we discussed above, the PA molecules might adopt a slightly twisted arrangement within cylindrical nanofibers and its handedness is determined by the chirality of β-sheet forming domain (Figure 1a).[29] The results obtained from a series of PA diastereomers indicate the possibility of supramolecular chiral recognition between PA assemblies with L-amino acid β-sheets, revealing a stronger affinity to (*R*)-phospholipid membranes than PAs with D-amino acid β-sheets. We also investigated their effect on hBMSC viabilities, and the CC50 values obtained for **L-V$_3$A$_3$-D-K$_3$** and **D-V$_3$A$_3$-L-K$_3$** were 57.91 μM and 58.97 μM, respectively (Figure S17). The diastereomers (**L-V$_3$A$_3$-D-K$_3$** and **D-V$_3$A$_3$-L-K$_3$**) showed intermediate cell viability compared to homochiral enantiomers (**L-V$_3$A$_3$-L-K$_3$**: CC50 = 54.71 μM; **D-V$_3$A$_3$-D-K$_3$**: CC50 = 65.14 μM). Similarly, we tried to understand the effect of supramolecular chirality on

DOI: 10.1021/acsbiomaterials.9b00553
ACS Biomater. Sci. Eng. XXXX, XXX, XXX−XXX

cell viabilities by comparing the CC50 values obtained for the diastereomers, however, because of the small magnitude of the effect we cannot conclude if these observations are directly linked to supramolecular chirality or not. We also cultured murine astroglial cells in the presence of diastereomer PAs, and the diastereomers showed intermediate cell viability compared to homochiral ones (Figure S15a). However, **L-V_3A_3-D-K_3** seemed to show lower cytotoxicity compared to **D-V_3A_3-L-K_3**. Namely, the cell viability of murine astroglial cells seems to be affected mainly by the chirality of the K_3 terminus rather than the chirality of V_3A_3 group. The observed differences among these two types of cells might be related to the difference in their membrane composition, particularly as related to charge.[38] Although beyond the scope of this paper, further studies may show that chirality effects in the extracellular matrix are highly dependent on the nature of specific cells.

CONCLUSIONS

We have demonstrated the chiral recognition of lipid bilayer membranes by supramolecular assemblies of PA molecules. Chiral recognition occurs at the interface of PA supramolecular assemblies and lipid membranes. We were also able to show that chiral recognition between these peptide assemblies, which have great potential as important therapies, and mammalian cells is a factor in mediating cell viability. Because supramolecular interactions are integral to many biological events, we anticipate that our study will not only provide a new strategy to design biomaterials but also contribute to our understanding of the origin of homochirality in nature.

ASSOCIATED CONTENT

Supporting Information

The Supporting Information is available free of charge on the ACS Publications website at DOI: 10.1021/acsbiomaterials.9b00553.

Details of synthesis, characterization, spectroscopic studies and experimental procedures (PDF)

AUTHOR INFORMATION

Corresponding Author

*Email: s-stupp@northwestern.edu.

ORCID

Kohei Sato: 0000-0002-8948-8537
Wei Ji: 0000-0002-1473-5222
Zaida Álvarez: 0000-0001-5104-1388
Liam C. Palmer: 0000-0003-0804-1168
Samuel I. Stupp: 0000-0002-5491-7442

Present Address

△K.S. is currently at Department of Life Science and Technology, Tokyo Institute of Technology, Yokohama, Japan 226-8501.

Author Contributions

The manuscript was written through contributions of all authors. All authors have given approval to the final version of the manuscript.

Funding

This work was supported by the Center for Bio-Inspired Energy Sciences (CBES), an Energy Frontiers Research Center (EFRC) funded by the U.S. Department of Energy, Office of Science, Office of Basic Energy Sciences, under Award DE-SC0000989, and by the Japan Society for the Promotion of Science (JSPS) through its "Grant-in-Aid for Research Activity Start-up" Grant 18H05971. Dr. Wei Ji is a postdoctoral fellow of the Research Foundation Flanders (12G2718N), and received a Travel Grant of Long Stay Abroad (V468915N) from the Research Foundation Flanders (FWO-Vlaanderen), and Junior Mobility Programme (JuMo) of KU Leuven (JUMO-15−0514). Dr. Z. Álvarez has received postdoctoral support from the Beatriu de Pinós Fellowship 2014 BP-A 00007 (Agència de Gestió d'Ajust Universitaris i de Recerca, (AGAUR), Spain), and by Grant PVA17_RF_0008 from the Paralyzed Veterans of America Research Foundation.

Notes

The authors declare no competing financial interest.

ACKNOWLEDGMENTS

We are grateful to the following core facilities at Northwestern University: Biological Imaging Facility and Keck Biophysics Facility for instrument use. This work made use of the EPIC facility of Northwestern University's NUANCE Center, which has received support from the Soft and Hybrid Nanotechnology Experimental (SHyNE) Resource (NSF NNCI-1542205); the MRSEC program (NSF DMR- 1121262) at the Materials Research Center; the International Institute for Nanotechnology (IIN); the Keck Foundation; and the State of Illinois, through the IIN. We acknowledge Dr. Reiner Bleher and Eric W. Roth (NUANCE/EPIC) for assistance with cryogenic TEM. This work made use of the IMSERC at Northwestern University, which has received support from the SHyNE Resource; the State of Illinois; and the IIN. Biological experiments were performed in the Analytical BioNanoTechnology Core Facility and peptide synthesis was performed in the Peptide Synthesis Core Facility, both of the Simpson Querrey Institute at Northwestern University. The U.S. Army Research Office, the U.S. Army Medical Research and Materiel Command, and Northwestern University provided funding to develop both of these facilities, and ongoing support is received from the SHyNE Resource. Portions of this work were performed at the DuPont-Northwestern-Dow Collaborative Access Team (DND-CAT) located at Sector 5 of the Advanced Photon Source (APS). DND-CAT is supported by Northwestern University, E.I. DuPont de Nemours & Co., and The Dow Chemical Company. This research used resources of the Advanced Photon Source, a U.S. Department of Energy (DOE) Office of Science User Facility operated for the DOE Office of Science by Argonne National Laboratory under Contract DE-AC02-06CH11357. Data was collected using an instrument funded by the National Science Foundation under Award 0960140. We acknowledge Dr. Steven Weigand for assistance with small-angle X-ray scattering (SAXS) measurements.

ABBREVIATIONS

PA, peptide amphiphile
HPLC, high-performance liquid chromatography
ESI, electrospray ionization
cryo-TEM, cryogenic transmission electron microscopy
SAXS, small-angle X-ray scattering
FT-IR, Fourier-transform infrared spectroscopy
CD, circular dichroism
DSC, differential scanning calorimetry
O.D., optical density
EC50, 50% effective concentration

DOI: 10.1021/acsbiomaterials.9b00553
ACS Biomater. Sci. Eng. XXXX, XXX, XXX−XXX

CC50, 50% cytotoxicity concentration.

REFERENCES

(1) Pasteur, L. Mémoire sur la Relation qui peut Exister Entre la Forme Cristalline et la Composition Chimique, et sur la Cause de la Polarisation Rotatoire. *C. R. Hebd. Seances Acad. Sci.* **1848**, *26*, 535−538.

(2) (a) Hegstrom, R. A.; Kondepudi, D. K. The Handedness of the Universe. *Sci. Am.* **1990**, *262*, 108−115. (b) Noyori, R. Asymmetric Catalysis: Science and Opportunities (Novel Lecture). *Angew. Chem., Int. Ed.* **2002**, *41*, 2008−2022. (c) Agranat, I.; Caner, H.; Caldwell, J. Putting Chirality to Work: The Strategy of Chiral Switches. *Nat. Rev. Drug Discovery* **2002**, *1*, 753−768. (d) Hembury, G. A.; Borovkov, V. V.; Inoue, Y. Chirality-Sensing Supramolecular Systems. *Chem. Rev.* **2008**, *108*, 1−73. (e) Wang, Y.; Xu, J.; Wang, Y.; Chen, H. Emerging Chirality in Nanoscience. *Chem. Soc. Rev.* **2013**, *42*, 2930−2962. (f) Yashima, E.; Ousaka, N.; Taura, D.; Shimomura, K.; Ikai, T.; Maeda, K. Supramolecular Helical Systems: Helical Assemblies of Small Molecules, Foldamers, and Polymers with Chiral Amplification and Their Functions. *Chem. Rev.* **2016**, *116*, 13752−13990. (g) Li, L.; Jiang, H.; Messmore, B. W.; Bull, S. R.; Stupp, S. I. A Torsional Strain Mechanism to Tune Pitch in Supramolecular Helices. *Angew. Chem., Int. Ed.* **2007**, *46*, 5873−5876.

(3) (a) Blackmond, D. G. The Origin of Biological Homochirality. *Cold Spring Harbor Perspect. Biol.* **2010**, *2*, a002147. (b) Budin, I.; Szostak, J. W. Expanding Roles for Diverse Physical Phenomena during the Origin of Life. *Annu. Rev. Biophys.* **2010**, *39*, 245−263.

(4) Yavin, E.; Yavin, Z. Attachment and Culture of Dissociated Cells from Rat Embryo Cerebral Hemispheres on Polylysine-Coated Surface. *J. Cell Biol.* **1974**, *62*, 540−546.

(5) Sun, T.; Han, D.; Rhemann, K.; Chi, L.; Fuchs, H. Stereospecific Interaction between Immune Cells and Chiral Surfaces. *J. Am. Chem. Soc.* **2007**, *129*, 1496−1497.

(6) Wang, X.; Gan, H.; Sun, T.; Su, B.; Fuchs, H.; Vestweber, D.; Butz, S. Stereochemistry Triggered Differential Cell Behaviors on Chiral Polymer Surfaces. *Soft Matter* **2010**, *6*, 3851−3855.

(7) Luo, Z.; Wang, S.; Zhang, S. Fabrication of Self-Assembling D-Form Peptide Nanofiber Scaffold D-EAK16 for Rapid Hemostasis. *Biomaterials* **2011**, *32*, 2013−2020.

(8) Wang, X.; Gan, H.; Zhang, M.; Sun, T. Modulating Cell Behaviors on Chiral Polymer Brush Films with Different Hydrophobic Side Groups. *Langmuir* **2012**, *28*, 2791−2798.

(9) Yao, X.; Hu, Y.; Cao, B.; Peng, R.; Ding, J. Effects of Surface Molecular Chirality on Adhesion and Differentiation of Stem Cells. *Biomaterials* **2013**, *34*, 9001−9009.

(10) Liu, G.-F.; Zhang, D.; Feng, C.-L. Control of Three-Dimensional Cell Adhesion by the Chirality of Nanofibers in Hydrogels. *Angew. Chem., Int. Ed.* **2014**, *53*, 7789−7793.

(11) Baranes, K.; Moshe, H.; Alon, N.; Schwartz, S.; Shefi, O. Neuronal Growth on L- and D-Cysteine Self-Assembled Monolayers Reveals Neuronal Chiral Sensitivity. *ACS Chem. Neurosci.* **2014**, *5*, 370−376.

(12) Appavu, R.; Chesson, C. B.; Koyfman, A. Y.; Snook, J. D.; Kohlhapp, F. J.; Zloza, A.; Rudra, J. S. Enhancing the Magnitude of Antibody Responses through Biomaterial Stereochemistry. *ACS Biomater. Sci. Eng.* **2015**, *1*, 601−609.

(13) Green, D. W.; Lee, J.−M.; Kim, E.−J.; Lee, D.−J.; Jung, H.−S. Chiral Biomaterials: From Molecular Design to Regenerative Medicine. *Adv. Mater. Interfaces* **2016**, *3*, 1500411−1500423.

(14) Zhang, M.; Qing, G.; Sun, T. Chiral Biointerface Materials. *Chem. Soc. Rev.* **2012**, *41*, 1972−1984.

(15) Zhao, X.; Xu, L.; Sun, M.; Ma, W.; Wu, X.; Xu, C.; Kuang, H. Tuning the Interactions between Chiral Plasmonic Films and Living Cells. *Nat. Commun.* **2017**, *8*, 2007.

(16) Wang, X.; Gan, H.; Sun, T. Chiral Design for Polymeric Biointerface: The Influence of Surface Chirality on Protein Adsorption. *Adv. Funct. Mater.* **2011**, *21*, 3276−3281.

(17) Lv, K.; Zhang, L.; Lu, W.; Liu, M. Control of Supramolecular Chirality of Nanofibers and Its Effect on Protein Adhesion. *ACS Appl. Mater. Interfaces* **2014**, *6*, 18878−18884.

(18) Gao, G.; Zhang, M.; Lu, P.; Guo, G.; Wang, D.; Sun, T. Chirality-Assisted Ring-Like Aggregation of Aβ(1−40) at Liquid-Solid Interfaces: A Stereoselective Two-Step Assembly Process. *Angew. Chem., Int. Ed.* **2015**, *54*, 2245−2250.

(19) (a) Pathirana, S.; Neely, W. C.; Myers, L. J.; Vodyanoy, V. Chiral Recognition of Odorants (+)- and (−)-Carvone by Phospholipid Monolayers. *J. Am. Chem. Soc.* **1992**, *114*, 1404−1405. (b) Bombelli, C.; Borocci, S.; Lupi, F.; Mancini, G.; Mannina, L.; Segre, A. L.; Viel, S. Chiral Recognition of Dipeptides in a Biomembrane Model. *J. Am. Chem. Soc.* **2004**, *126*, 13354−13362. (c) Ishigami, T.; Suga, K.; Umakoshi, H. Chiral Recognition of L-Amino Acids on Liposomes Prepared with L-Phospholipid. *ACS Appl. Mater. Interfaces* **2015**, *7*, 21065−21072.

(20) (a) Hartgerink, J. D.; Beniash, E.; Stupp, S. I. Self-Assembly and Mineralization of Peptide-Amphiphile Nanofibers. *Science* **2001**, *294*, 1684−1688. (b) Hendricks, P. M.; Sato, K.; Palmer, L. C.; Stupp, S. I. Supramolecular Assembly of Peptide Amphiphiles. *Acc. Chem. Res.* **2017**, *50*, 2440−2448.

(21) (a) Ortony, J. H.; Newcomb, C. J.; Matson, J. B.; Palmer, L. C.; Doan, P. E.; Hoffman, B. M.; Stupp, S. I. Internal Dynamics of a Supramolecular Nanofibre. *Nat. Mater.* **2014**, *13*, 812−816. (b) Tantakitti, F.; Boekhoven, J.; Wang, X.; Kazantsev, R. V.; Yu, T.; Li, J.; Zhuang, E.; Zandi, R.; Ortony, J. H.; Newcomb, C. J.; Palmer, L. C.; Shekhawat, G. S.; de la Cruz, M. O.; Schatz, G. C.; Stupp, S. I. Energy Landscapes and Functions of Supramolecular Systems. *Nat. Mater.* **2016**, *15*, 469−476. (c) Da Silva, R. M. P.; Van der Zwaag, D.; Albertazzi, L.; Lee, S. S.; Meijer, E. W.; Stupp, S. I. Super Resolution Microscopy Reveals Structural Diversity in Molecular Exchange among Peptide Amphiphile Nanofibres. *Nat. Commun.* **2016**, *7*, 11561.

(22) Silva, G. A.; Czeisler, C.; Niece, K. L.; Beniash, E.; Harrington, D. A.; Kessler, J. A.; Stupp, S. I. Selective Differentiation of Neural Progenitor Cells by High-Epitope Density Nanofibers. *Science* **2004**, *303*, 1352−1355.

(23) Tysseling-Mattiace, V. M.; Sahni, V.; Niece, K. L.; Birch, D.; Czeisler, C.; Fehlings, M. G.; Stupp, S. I.; Kessler, J. A. Self-Assembling Nanofibers Inhibit Glial Scar Formation and Promote Axon Elongation after Spinal Cord Injury. *J. Neurosci.* **2008**, *28*, 3814−3823.

(24) Sato, K.; Hendricks, M. P.; Palmer, L. C.; Stupp, S. I. Peptide Supramolecular Materials for Therapeutics. *Chem. Soc. Rev.* **2018**, *47*, 7539−7551.

(25) Lee, S. S.; Hsu, E. L.; Mendoza, M.; Ghodasra, J.; Nickoli, M. S.; Ashtekar, A.; Polavarapu, M.; Babu, J.; Riaz, R. M.; Nicolas, J. D.; Nelson, D.; Hashmi, S. Z.; Kaltz, S. R.; Earhart, J. S.; Merk, B. R.; McKee, J. S.; Bairstow, S. F.; Shah, R. N.; Hsu, W. K.; Stupp, S. I. Gel Scaffolds of BMP-2-Binding Peptide Amphiphile Nanofibers for Spinal Arthrodesis. *Adv. Healthcare Mater.* **2015**, *4*, 131−141.

(26) Guler, M. O.; Soukasene, S.; Hulvat, J. F.; Stupp, S. I. Presentation and Recognition of Biotin on Nanofibers Formed by Branched Peptide Amphiphiles. *Nano Lett.* **2005**, *5*, 249−252.

(27) Newcomb, C. J.; Sur, S.; Ortony, J. H.; Lee, O.-S.; Matson, J. B.; Boekhoven, J.; Yu, J. M.; Schatz, G. C.; Stupp, S. I. Cell Death versus Cell Survival Instructed by Supramolecular Cohesion of Nanostructures. *Nat. Commun.* **2014**, *5*, 3321.

(28) Ortony, J. H.; Qiao, B.; Newcomb, C. J.; Keller, T. J.; Palmer, L. C.; Deiss-Yehiely, E.; Olvera de la Cruz, M.; Han, S.; Stupp, S. I. Water Dynamics from the Surface to the Interior of a Supramolecular Nanostructure. *J. Am. Chem. Soc.* **2017**, *139*, 8915−8921.

(29) Nesloney, C. L.; Kelly, J. W. Progress towards Understanding β-Sheet Structure. *Bioorg. Med. Chem.* **1996**, *4*, 739−766.

(30) Springs, B.; Haake, P. Equilibrium Constants for Association of Guanidinium and Ammonium Ions with Oxyanions: The Effect of Changing Basicity of the Oxyanion. *Bioorg. Chem.* **1977**, *6*, 181−190.

DOI: 10.1021/acsbiomaterials.9b00553
ACS Biomater. Sci. Eng. XXXX, XXX, XXX−XXX

(31) Sato, K.; Ji, W.; Palmer, L. C.; Weber, B.; Barz, M.; Stupp, S. I. Programmable Assembly of Peptide Amphiphile via Noncovalent-to-Covalent Bond Conversion. *J. Am. Chem. Soc.* **2017**, *139*, 8995−9000.
(32) Leventis, P. A.; Grinstein, S. The Distribution and Function of Phosphatidylserine in Cellular Membranes. *Annu. Rev. Biophys.* **2010**, *39*, 407−427.
(33) Jurkiewicz, P.; Cwiklik, L.; Vojtíšková, A.; Jungwirth, P.; Hof, M. Structure, Dynamics, and Hydration of POPC/POPS Bilayers Suspended in NaCl, KCl, and CsCl Solutions. *Biochim. Biophys. Acta, Biomembr.* **2012**, *1818*, 609−616.
(34) Guidotti, G.; Brambilla, L.; Rossi, D. Cell-Penetrating Peptides: From Basic Research to Clinics. *Trends Pharmacol. Sci.* **2017**, *38*, 406−424.
(35) Åkesson, A.; Lundgaard, C. V.; Ehrlich, N.; Pomorski, T. G.; Stamou, D.; Cárdenas, M. Induced Dye Leakage by PAMAM G6 does not Imply Dendrimer Entry into Vesicle Lumen. *Soft Matter* **2012**, *8*, 8972−8980.
(36) Lee, D.-W.; Kim, T.; Park, I.-S.; Huang, Z.; Lee, M. Multivalent Nanofibers of a Controlled Length: Regulation of Bacterial Cell Agglutination. *J. Am. Chem. Soc.* **2012**, *134*, 14722−14725.
(37) Pazos, E.; Sleep, E.; Rubert Pérez, C. M.; Lee, S. S.; Tantakitti, F.; Stupp, S. I. Nucleation and Growth of Ordered Arrays of Silver Nanoparticles on Peptide Nanofibers: Hybrid Nanostructures with Antimicrobial Properties. *J. Am. Chem. Soc.* **2016**, *138*, 5507−5510.
(38) Spector, A. A.; Yorek, M. A. Membrane Lipid Composition and Cellular Function. *J. Lipid Res.* **1985**, *26*, 1015−1035.
(39) McNeil, P. L.; Steinhardt, R. A. Loss, Restoration, and Maintenance of Plasma Membrane Integrity. *J. Cell Biol.* **1997**, *137*, 1−4.

DOI: 10.1021/acsbiomaterials.9b00553
ACS Biomater. Sci. Eng. XXXX, XXX, XXX−XXX